

1 Rates and drivers of Red Sea plankton community metabolism

2 Daffne C. López-Sandoval¹, Katherine Rowe¹, Paloma Carillo-de-Albonoz¹, Carlos M. Duarte¹ and

3 Susana Agustí¹

4 ¹ Red Sea Research Center, King Abdullah University of Science and Technology (KAUST), Thuwal-Jeddah, 23955-6900,

5 Saudi Arabia

6 *Correspondence to:* Daffne C. López-Sandoval (daffne.lopezsandoval@kaust.edu.sa)

7 Abstract

8 Resolving the environmental drivers shaping planktonic communities is fundamental to understanding
9 their variability, in the present and the future, across the ocean. More specifically, addressing the
10 temperature-dependence response of planktonic communities is essential as temperature plays a key
11 role in regulating metabolic rates, thus potentially defining the ecosystem functioning. Here we
12 quantified plankton metabolic rates along the Red Sea, a uniquely oligotrophic and warm environment,
13 and analysed the drivers that regulate gross primary production (GPP), community respiration (CR) and
14 net community production (NCP). The study was conducted on six oceanographic surveys following a
15 north-south transect along the Saudi Arabian coast. Our findings revealed that GPP and CR rates
16 increased with increasing temperature ($R^2 = 0.41$ and 0.19 , respectively, $p < 0.001$ in both cases), with a
17 higher activation energy (E_a) for GPP (1.20 ± 0.17 eV) than for CR (0.73 ± 0.17 eV). The higher E_a for
18 GPP than for CR resulted in a positive relationship between NCP and temperature. This unusual
19 relationship is likely driven by 1) the relatively higher nutrient availability found towards the warmer
20 region (i.e., the south of the Red Sea), which favours GPP rates above the threshold that separates
21 autotrophic from heterotrophic communities ($1.7 \text{ mmol O}_2 \text{ m}^{-3} \text{ d}^{-1}$) in this region. 2) Due to the arid
22 nature, the basin lacks riverine and terrestrial inputs of organic carbon to subsidise a higher metabolic
23 response of heterotrophic communities, thus constraining CR rates. Our study suggests that GPP

24 increases steeply with increasing temperature in the warm ocean when relatively high nutrient inputs are
25 present.

26 **1 Introduction**

27 The balance between gross primary production and community respiration, which involves both
28 autotrophic and heterotrophic metabolic activity (Williams, 1993; Cullen, 2001; Ducklow and Doney,
29 2013), sets the metabolic status of an ecosystem by defining the carbon available to fuel pelagic food
30 webs and determining whether plankton communities act as a source or sink of CO₂ (Del Giorgio et al.,
31 1997; Williams, 1998). Whereas GPP typically satisfies the respiratory demands within the food web
32 across productive waters, the oligotrophic ocean often requires allochthonous inputs of organic carbon
33 to meet the metabolic requirements of heterotrophic organisms (Smith and Mackenzie, 1987). Due to
34 comparatively higher carbon consumption, relative to the production, planktonic communities in low
35 productivity systems are in close metabolic balance (i.e., $NCP = 0$, or $GPP = CR$) or experience a net
36 metabolic imbalance (i.e. $NCP < 0$, $GPP < CR$) (Smith and Hollibaugh, 1993; Duarte and Agustí, 1998;
37 Duarte et al., 2013).

38 In tropical and subtropical oligotrophic regions, the high temperatures may amplify the
39 metabolic imbalances in plankton communities, as CR tends to increase faster than GPP (Harris et al.,
40 2006; Regaudie-de-Gioux and Duarte, 2012) if the allochthonous sources of organic carbon are enough
41 to subsidise their carbon demand. These allochthonous inputs may be delivered from land through
42 riverine discharge, from the atmosphere through atmospheric deposition of dust and volatile organic

43 carbon (Jurado et al., 2008), or are exported from productive coastal habitats (Duarte et al., 2013;
44 Barrón and Duarte, 2015).

45 The Red Sea is a semi-enclosed highly oligotrophic basin (Acker et al., 2008; Raitzos et al.,
46 2013). It is known as one of the warmest tropical seas, with maximum sea surface temperatures ranging
47 from 33.0 to 33.9 °C during summer (Chaidez et al., 2017; Osman et al., 2018), and up to 34–35 °C in
48 certain parts of the basin (Rasul and Stewart, 2015; Garcias-Bonet and Duarte, 2017; Almahasheer et
49 al., 2018). Due to the prevailing arid conditions, the Red Sea experiences large evaporation rates (nearly
50 2 cm yr⁻¹ of freshwater from the surface layers), while the lack of river runoff and low precipitation
51 rates make this system one of the saltiest seas on the planet (Sofianos, 2002; Sofianos and Johns, 2015;
52 Zarokanellos et al., 2017). Two wind patterns govern the region: in the northern part, the wind coming
53 from the northwest remains relatively constant throughout the year, while in the southern area, the
54 Indian Monsoon system regulates the wind dynamics (Sofianos, 2002; Sofianos and Johns, 2015).
55 During the winter monsoon, the wind changes direction, and this wind reversal along with the
56 thermohaline forces drives the overall circulation and favours the exchange of water with the Indian
57 Ocean (Sofianos, 2002; Zarokanellos et al., 2017).

58 Due to the almost negligible terrestrial inputs, the intrusion of nutrient-rich waters from the
59 Indian Ocean through the Bab-el-Mandeb Strait (Sofianos and Johns, 2007; Raitzos et al., 2015; Kürten
60 et al., 2016), together with aeolian dust and aerosol deposition (Chen et al., 2007; Engelbrecht et al.,
61 2017), represent the primary sources of nutrients into the basin. Thus, nutrient availability in the Red
62 Sea follows a latitudinal pattern that is opposite to the one of salinity, but parallel to the thermal

63 gradient, with nutrient-richer and warmer waters towards the Southern Red Sea compared to the cooler
64 and more oligotrophic Northern Red Sea (Sofianos, 2002; Raitzos et al., 2015).

65 Studies based on ocean color data revealed that chlorophyll-a (Chl-a) concentrations decline
66 from the Southern Red Sea to the Northern Red Sea (Raitzos et al., 2013; Kheireddine et al., 2017;
67 Qurban et al., 2017) and depict a clear seasonality. During winter time, when the maximum exchange of
68 water with the Indian Ocean takes place, Chl-a concentration peaks, decreasing towards the summer
69 period when the water column is mostly stratified (Sofianos, 2002). Measurements of primary
70 production also revealed that phytoplankton photosynthetic rates follow the same south to north
71 gradient as Chl-a and nutrient concentration (Qurban et al., 2017; López-Sandoval et al., 2019).
72 However, reports regarding the metabolic balance of the plankton communities are scarce, mostly focus
73 on the contribution of the autotrophic community via photosynthetic processes (Levanon-Spanier et al.,
74 1979; Qurban et al., 2014; Rahav et al., 2015), or are restricted to specific regions (Tilstra et al., 2018).

75 Based on available evidence, we hypothesise that the high gross primary production expected in
76 the Southern Red Sea may be counterbalanced by a higher respiratory demand in these warm waters,
77 and that NCP might decline towards the relatively unproductive waters of the Northern Red Sea. With
78 the expected decrease in GPP towards the northern region, planktonic metabolism might be driven
79 mainly by heterotrophic communities (Duarte and Agustí, 1998; Duarte et al., 2013). However, the
80 absence of significant allochthonous subsidies in the basin may hamper the metabolic response of the
81 heterotrophic plankton communities. Hence, it remains unclear what the metabolic balance of plankton
82 communities is and whether a south to north latitudinal gradient in NCP exists in the Red Sea.

83 Here we report the variability of plankton community metabolism (GPP, CR and NCP) along a
84 latitudinal gradient in the Red Sea, and examine if the temperature-dependence of planktonic metabolic
85 rates in this basin are consistent with those reported for the global ocean (López-Urrutia et al., 2006;
86 Regaudie-de-Gioux and Duarte, 2013; Garcia-Corral et al., 2017). We did so by conducting
87 measurements as part of six surveys along the south-north latitudinal gradient in the Saudi Economic
88 Exclusive Zone in Red Sea waters. Specifically, we determined plankton metabolic rates between
89 winter 2016 and spring 2018, thus allowing us to 1) delineate the seasonal variability of the gross
90 primary production and community respiration along the Red Sea, 2) quantify changes in the metabolic
91 balance (net community production) and 3) test the hypothesized roles of productivity gradients and
92 temperature in driving NCP.

93 **2. Material and Methods**

94 **2.1 Field Sampling**

95 We conducted six oceanographic surveys: two during autumn (October and November 2016),
96 two during winter (February 2016 and January 2017), one in summer (August 2017), and one in spring
97 (March 2018) on board the R/V *Thuwal* and R/V *Al Azizi*. Sampling was conducted following a
98 latitudinal transect along the Red Sea within a region limited by coordinates 17.25 °N to 27.82 °N and
99 34.83 °E to 41.39 °E (Figure 1). At each station, vertical profiles of temperature and salinity were
100 obtained with a Sea-Bird SBE 911 plus CTD profiler (Sea-Bird Electronics, Bellevue, WA, USA),
101 equipped with additional sensors to measure the attenuation of photosynthetically active radiation
102 (PAR) (Biospherical/Licor PAR/Irradiance Sensor), *in vivo* fluorescence (WetLabs ECO FL
103 fluorometer), and dissolved oxygen concentration (Sea-Bird SBE 43 Dissolved Oxygen Sensor). Water
104 samples for chemical and biological measurements were collected between 7:00 and 9:00 am local time,
105 using a rosette sampler equipped with 12 Teflon Niskin bottles (12 L) that were provided with silicone
106 O-rings and seals.

107 **2.2 Inorganic nutrients and chlorophyll-a concentration**

108 Water samples for nutrient analyses were collected in 50 mL polyethylene bottles and kept frozen
109 (-20 °C) until further processing. Inorganic nutrient concentration was determined with a SEAL AA3
110 Segmented Flow Analyzer (SEAL Analytical Inc., WI, USA) using standard methods (Hansen and
111 Koroleff, 1999). The detection limits were 0.05 µM for nitrate, 0.01 µM for nitrite, 0.01 µM for

112 phosphate and 0.08 μM for silicate. For the chlorophyll-a analysis, 200 mL samples were taken at ten
113 discrete depths (between 5 and 200 m) and filtered through Whatman GF/F filters. The filters were kept
114 frozen (-20 °C) until further analysis. Pigments were extracted for 24 h using 90 % acetone and left
115 overnight in the dark at 4 °C. Chl-a concentration was estimated with the non-acidification technique
116 using a Trilogy Fluorometer equipped with CHL-NA module (Turner Designs, San Jose, USA),
117 previously calibrated with pure Chl-a.

118 **2.3 Net community metabolism, community respiration and gross primary production**

119 Plankton metabolic rates were determined *in vitro* by measuring the changes in dissolved
120 oxygen concentration after 24 h light-dark bottle (Winkler) incubations (Carpenter, 1965). This
121 methodology, commonly used to determine plankton metabolic rates (Williams et al., 1979; Duarte and
122 Agustí, 1998; Bender et al., 1999; Robinson and Williams, 1999; Ducklow et al., 2000; Serret et al.,
123 2001; Robinson et al., 2002; Serret et al., 2009; García-Martín et al., 2017), allows to account for the
124 diel cycle of oxygen and carbon fluxes derived from photosynthetic mechanisms (light-dependent
125 reactions) and also those linked to the acquisition of energy by both autotrophic and heterotrophic
126 microorganisms (light and dark-dependent reactions) (Robinson and Williams, 2005; Williams and del
127 Giorgio, 2005).

128 Water samples were collected at three different optical depths (ζ) through the water column.
129 One at the surface (100–80 % of incident PAR), another towards the bottom of the photic layer (8–1 %
130 of incident PAR), and one intermediate sample, at a depth of the chlorophyll maximum (Chl-*a* max). In
131 case the Chl-*a* max was sampled at the surface or bottom layers, the intermediate sample was taken

132 between 1.5–2.3 ζ (i.e., 22–10 % of incident PAR). Seawater was collected directly from the Niskin
133 bottles to fill a total of 21 (100 mL) Winkler bottles. The bottles were carefully filled using silicone
134 tubing and allowing the water to overflow during the filling, taking special care to avoid the formation
135 of air bubbles. Surface samples were collected in 100 mL quartz bottles. From each depth, seven of the
136 bottles were immediately fixed with Manganese sulphate (MnSO_4) and Potassium hydroxide/Potassium
137 iodide solution (KI/KOH) to determine the initial oxygen concentration while the other 14, seven light
138 and seven black bottles, were incubated on deck in surface water flow-through tanks. Due to the
139 difference in temperature between the surface and deep waters, particularly during the summer and
140 autumn surveys, we decided to include in our analyses only those samples collected above the
141 thermocline. Changes in temperature and PAR in the incubation tanks were recorded with HOBO
142 Pendant data loggers (Onset, Massachusetts, USA).

143 Before the incubation, the bottles were covered with neutral mesh to reduce the incident PAR
144 radiation according to the sampled depth. At the end of the incubation period, light and dark bottles
145 from each depth were fixed to determine final O_2 concentrations. Oxygen concentration was measured
146 by automated high-precision Winkler titration with a potentiometric end-point detection (Oudot et al.,
147 1988) using a Mettler Toledo T50 Titration Excellence auto-titrator attached to an Inmotion
148 autosampler. NCP was calculated as the difference in the oxygen concentration between the light bottles
149 after the 24 h incubation period ($[\text{O}_2]_{\text{L-24h}}$) and the oxygen concentration measured before the
150 incubation ($[\text{O}_2]_{\text{Tzero}}$) (i.e., $\text{NCP} = ([\text{O}_2]_{\text{L-24h}} - [\text{O}_2]_{\text{Tzero}})$). CR rates ($\text{mmol O}_2 \text{ m}^{-3} \text{ d}^{-1}$) were calculated as
151 the difference of the oxygen concentration after the 24 h incubation period in the dark bottles ($[\text{O}_2]_{\text{D}}$).

152 $_{24h}$) and the initial oxygen concentration ($[O_2]_{Tzero}$) (i.e., $CR = [O_2]_{Tzero} - ([O_2]_{D-24h})$). GPP ($\text{mmol O}_2 \text{ m}^{-3} \text{ d}^{-1}$) was calculated as the sum of NCP and CR.

154 Due to the consistent relationship existing between plankton metabolism and temperature across
155 diverse marine regions (Regaudie-de-Gioux and Duarte, 2012; García-Corral et al., 2014), we examined
156 how plankton metabolic rates covariate with temperature in the Red Sea, a system whose temperature
157 range is higher than previously encountered in marine planktonic metabolism research. We determined
158 the relationship between metabolic rates and temperature by fitting an ordinary least squares linear
159 regression equation to the relationship between the natural logarithm of the Chl-a specific metabolic
160 rates (B_0) and the inverse of the absolute temperature * k (i.e., $1/kT$), where k is the Boltzmann's
161 constant ($8.617734 * 10^{-5} \text{ eV K}^{-1}$) (Gillooly et al., 2001; Brown et al., 2004):

$$162 \quad \text{Ln } B_0 = -Ea(1/kT) + C \quad (1)$$

163 In these so-called Arrhenius plots, the slope of this relationship represents the average activation energy
164 ($Ea = -\text{slope}$), characterising the extent of thermal-dependence of metabolic processes.

165 **2.4 Statistical analyses**

166 Statistical analyses and figures were done using the statistical and machine learning toolbox in
167 Matlab version R2018b (Mathworks Inc, Natick, MA, USA) and with the R statistical computing
168 package using RStudio 1.1419. Pearson correlation tests were used (corrplot function in R) to determine
169 the relationship between environmental variables (temperature, nitrate + nitrite (NOx), phosphate and
170 silicate concentration) and their latitudinal distribution, and to determine the relationship between
171 volumetric measurements of GPP, CR, NCP, and environmental variables (Temperature, NOx

172 concentration, Chl-*a*, and latitude). We used ordinary least squares (OLS) simple regression models
173 (fitlm function in Matlab) to describe the potential relationships between different planktonic metabolic
174 rates, between metabolic rates and environmental variables, and to predict the response of the Chl-*a*
175 normalised GPP (and CR) to temperature (Arrhenius plots described in section 2.3). To test if the
176 activation energies (obtained from the Arrhenius plots) were significantly different, we performed an
177 analysis of covariance (ANCOVA) by using the aocool in Matlab. The variability of planktonic
178 metabolic rates between cruises was statistically analysed using non-parametric Kruskal-Wallis tests.
179 Mean values and their standard error of the mean (SE) are reported throughout the text.

180 **3. Results**

181 **3.1 Latitudinal variability of physico-chemical properties and Chl-*a* concentration**

182 Hydrographic (temperature and salinity) and chemical variables (nutrient concentrations)
183 depicted a marked latitudinal gradient typical of the Red Sea. At the southern-most area, sea surface
184 temperature (SST) fluctuated between 28 °C (winter-spring) and 32 °C (summer), while at the far-
185 northern sampling site SST ranged between 23 °C (winter) and 27–28 °C (summer-autumn) (Figure 2).
186 Overall, all macronutrients observed a significant inverse correlation with latitude (Pearson correlation
187 coefficients $r < -0.4$, $p < 0.05$) (Figure 3). Nitrite+nitrate (NO_x) decreased from $6.1 \pm 0.9 \mu\text{M}$ in the
188 southern region to $2.9 \pm 0.3 \mu\text{M}$ towards the northern Red Sea, while on average, phosphate
189 concentration ranged from $0.5 \pm 0.01 \mu\text{M}$ in the south of the Red Sea to $0.1 \pm 0.01 \mu\text{M}$ towards the
190 northern stations (data not shown). Phytoplankton biomass (measured as Chl-*a* concentration) also

191 decreased significantly towards the north of the Red Sea (Pearson's correlation, $r = -0.4$, $p < 0.001$, $n =$
192 77) (Table 1). We found the highest autotrophic biomass during the autumn and winter cruises. During
193 this period, surface Chl-a ranged from 0.6–0.8 mg m^{-3} in the southern region to 0.2–0.3 mg m^{-3} in the
194 north (Figure 2). In general, our results confirm that all variables correlated significantly with latitude,
195 highlighting the prevalence of the south-north gradient in temperature, salinity, nutrient availability and
196 chlorophyll-a concentration across the Red Sea.

197 **3.2 Variability of plankton metabolism measured along the Red Sea**

198 Analogous to the environmental variability, planktonic metabolism followed the same
199 significant north-south decreasing pattern with latitude (Figure 4). The inverse correlation of GPP rates
200 with latitude was highly significant (Pearson correlation coefficient $r = -0.6$, $p < 0.001$, $n = 77$) (Table
201 1), as found for autotrophic biomass, thus, explaining the strong correlation observed between GPP and
202 Chl-a concentration (Pearson correlation coefficient $r = 0.7$, $n = 77$) (Table 1). GPP rates decreased on
203 average by 79%, from $4.1 \pm 0.5 \text{ mmol O}_2 \text{ m}^{-3} \text{ d}^{-1}$ ($\approx 49.2 \text{ mgC m}^{-3} \text{ d}^{-1}$; assuming a photosynthetic
204 quotient, $\text{PQ} = 1$) at the southernmost station of the Red Sea to 0.9 ± 0.1 ($\approx 10 \text{ mgC m}^{-3} \text{ d}^{-1}$; $\text{PQ} = 1$) at
205 the northern site, while CR decreased on average by 73 %, from $3 \pm 0.4 \text{ mmol O}_2 \text{ m}^{-3} \text{ d}^{-1}$ ($\approx 36 \text{ mgC m}^{-3}$
206 d^{-1} ; assuming a respiratory quotient, $\text{RQ} = 1$) in the south to 0.8 ± 0.1 in the north ($\approx 9.6 \text{ mgC m}^{-3} \text{ d}^{-1}$;
207 $\text{RQ} = 1$) (Figure 4). We did not find any significant correlation between NO_x availability and GPP
208 (Pearson correlation coefficient, $p > 0.05$, $n = 56$), CR (Pearson correlation coefficient, $r = 0.2$, $p > 0.05$)
209 nor NCP rates (Pearson correlation coefficient, $r = -0.2$, $p > 0.05$, $n = 56$) (Table 1); however, all
210 metabolic rates were positively correlated with temperature (Table 1).

211 The highest GPP and CR rates measured along the Red Sea came from data collected during the
212 autumn and winter cruises, when GPP and CR rates reached values above 6 and 4 mmol O₂ m⁻³ d⁻¹,
213 respectively (Figure 5), and when the mean values were the highest (GPP_{autumn-winter} = 2.9 ± 0.3 – 2.3 ±
214 0.3 mmol O₂ m⁻³ d⁻¹; CR_{autumn-winter} = 2.5 ± 0.3 – 2 ± 0.2) (Figure 5). However, despite the overall
215 variability between autumn-winter and spring-summer, when all data are taken in concert, planktonic
216 GPP and CR rates were not significantly different between seasons (Kruskal-Wallis H test, $\chi^2 = 6.83$, p
217 = 0.08; $\chi^2 = 4.14$, p = 0.25, respectively). Furthermore, the balance between planktonic autotrophic
218 production (GPP) and respiratory losses (due to the heterotrophic and autotrophic metabolism, CR) (i.e.,
219 NCP rates) revealed that NCP rates also decreased towards the northern region (by 94%). From 1.1 ±
220 0.3 mmol O₂ m⁻³ d⁻¹ at the southern stations to 0.1 ± 0.1 mmol O₂ m⁻³ d⁻¹ above 26 °N (Figure 4). The
221 average NCP measured during our cruises was 0.3 ± 0.1 mmol O₂ m⁻³ d⁻¹ (Figure 5), which indicates an
222 overall prevalence of autotrophic communities (Figure 5). However, a closer look at our data revealed
223 the mean NCP rate in spring was -0.3 ± 0.2 mmol O₂ m⁻³ d⁻¹ (Figure 5), while during summer, NCP
224 rates in the northern region ranged from -0.6 to -0.1 mmol O₂ m⁻³ d⁻¹, which evidenced that planktonic
225 metabolism was governed by heterotrophic communities during both spring and summer in the northern
226 region.

227 When we evaluated the relationship of GPP with CR and NCP, the analysis showed that both
228 CR and NCP increased significantly with GPP ($R^2 = 0.62$ and 0.49, respectively; p < 0.001) (Figure 6).
229 From the functional relationships between GPP with CR and NCP, we calculated the threshold of GPP
230 for metabolic equilibrium for the region. By solving for GPP = CR and for NCP = 0 (from the
231 relationship describing NCP as a function of GPP), and by using the slope and intercept shown in

232 figures 6A and 6B, we determined that the GPP threshold that separates autotrophic from heterotrophic
233 planktonic communities in the Red Sea is $1.7 \text{ mmol O}_2 \text{ m}^{-3} \text{ d}^{-1}$ (range 1.2–1.9 $\text{mmol O}_2 \text{ m}^{-3} \text{ d}^{-1}$).

234 **3.3 Metabolic rates and temperature**

235 Due to the pervasive influence of temperature in regulating metabolic rates, we further explored
236 the temperature-dependence of GPP and CR by analysing the relationship between chlorophyll-a
237 specific metabolic rates and temperature. Our analysis revealed that both GPP and CR tended to
238 increase with temperature albeit with different activation energies (i.e., E_a was significantly higher for
239 GPP ($1.20 \pm 0.17 \text{ eV}$) than for CR rates ($0.73 \pm 0.17 \text{ eV}$), ANCOVA, $F = 3.96$, $p = 0.04$) (Figure 7). We
240 also tested whether the temperature-dependence response was consistent between cruises (Figure 8).
241 Our results indicated a relatively higher activation energy for GPP during the summer cruise ($2.31 \pm$
242 0.75 eV) and for CR in spring ($2.60 \pm 0.85 \text{ eV}$). However, the observed differences in the activation
243 energies for GPP were not significantly different between seasons (ANCOVA, $F = 0.38$, $p = 0.8$).

244

245 4. Discussion

246 4.1 Variability of plankton community metabolic rates along the Red Sea

247 Our results demonstrate that planktonic metabolic rates are markedly different between the
248 southern and northern regimes of the Red Sea, with a northward increase in the overall mean GPP and
249 CR by a factor of 5 and 4, respectively (i.e., an absolute increase in GPP rates of $3.2 \text{ mmol O}_2 \text{ m}^{-3} \text{ d}^{-1} \approx$
250 $38.4 \text{ mgC m}^{-3} \text{ d}^{-1}$, while absolute CR rates increased by $2.2 \text{ mmol O}_2 \text{ m}^{-3} \text{ d}^{-1} \approx 26.4 \text{ mgC m}^{-3} \text{ d}^{-1}$).

251 Although, *sensu stricto*, the overall balance between autotrophic metabolism and planktonic community
252 respiration (i.e. NCP) indicated a prevalence of autotrophic communities during our samplings along the
253 Red Sea, heterotrophic communities prevailed during the spring, and in the northern stations during the
254 summer, which highlights the shift in the trophic conditions in the basin. Consistent with these findings,
255 our data revealed that the GPP threshold that separated autotrophic from heterotrophic communities in
256 the Red Sea ($1.7 \text{ mmol O}_2 \text{ m}^{-3} \text{ d}^{-1}$) is similar to that reported across oceanic communities elsewhere
257 (Duarte and Agustí, 1998; Duarte and Regaudie-de-Gioux, 2009), agreeing with the oligotrophic
258 characteristics that govern the basin at certain periods or locations. The latitudinal differences depicted
259 in our results mirror the increasing north-south pattern in Chl-*a* concentration and photosynthetic carbon
260 fixation rates previously reported for the Red Sea (Acker et al., 2008; Raitzos et al., 2013; Qurban et al.,
261 2014; Kheireddine et al., 2017), and which are supported by the presence of different planktonic
262 communities (Al-aidaroos et al., 2016; Pearman et al., 2016; Robitzch et al., 2016; Kheireddine et al.,
263 2017; Kottuparambil and Agusti, 2018).

264

265 The lower productivity of the northern section of the Red Sea explains the dominance of
266 heterotrophic communities therein. Still, sustaining heterotrophy in oligotrophic regions requires an
267 allochthonous source of organic matter (Duarte et al. 2011, 2013). The arid nature of the northern Red
268 Sea, with the watershed consisting mostly of deserts, leads to the absence of rivers and significant
269 organic carbon inputs to the sea. Dust inputs are important, however, and whereas they have shown no
270 effect on primary production (Torfstein and Kienast, 2018), they are a source of organic carbon (Jurado
271 et al. 2009) that can partially supply the organic matter required to sustain heterotrophic communities.
272 Moreover, the Red Sea supports highly productive coral reefs, mangrove forests, seagrass meadows and
273 algal communities in its extensive shallow coastal areas (Rasul et al., 2015; Almahasheer et al., 2016),
274 which may export significant organic carbon to the pelagic compartment, thereby helping to sustain
275 heterotrophic plankton communities in the northern Red Sea.

276 **4.2 Temperature and metabolic balance in the Red Sea**

277 Temperature is a master variable that regulates many components of ocean dynamics, such as
278 vertical stratification and most aspects of organismal biology, from setting boundaries in the distribution
279 of organisms (Clarke, 1996) to controlling biochemical reactions that constrain the energy for metabolic
280 processes (Gillooly et al., 2001). Hence, temperature is likely a significant driver of metabolic processes
281 in the Red Sea, one of the warmest tropical marine ecosystems (Raitsos et al., 2011; Chaidez et al.,
282 2017). Indeed, our results showed a positive response of planktonic metabolism to temperature.
283 Moreover, the functional relationships between metabolic rates with temperature suggested that both
284 GPP and CR were positively enhanced with increasing temperature; but at a different pace.

285 The metabolic theory of ecology (MTE) relates the metabolic rate of an organism with its mass
286 and temperature. This theory hypothesizes that individual metabolic rates relate to temperature with a
287 relatively constant activation energy ($E_a \sim 0.63$ eV) for a wide range of taxa, from unicellular organisms
288 to plants and animals (Gillooly et al., 2001; Brown et al., 2004). For aerobic respiration, E_a values vary
289 between 0.41 and 0.74 eV at temperatures between 0–40 °C (Gillooly et al., 2005), while for
290 photosynthetic processes, the predicted E_a is lower, ~ 0.32 eV (Allen et al., 2005). From a thorough
291 compilation of data obtained for a wide range of marine systems (from polar to subtropical and tropical
292 oceanic regions), Regaudie-de-Gioux and Duarte (2012) found that overall, the activation energies for
293 photosynthetic production (GPP) varied between 0.29–0.32 eV, and for respiratory processes (CR)
294 between 0.65 and 0.66 eV.

295 The E_a for GPP (1.20 ± 0.17 eV) obtained for the Red Sea was higher than the overall value
296 predicted by the MTE, while the E_a values for CR were below those for GPP (0.72 ± 0.17 eV) unlike
297 observed elsewhere in open oceanic waters (Regaudie-de-Gioux and Duarte 2011, Garcia-Corral et al.
298 2017). Furthermore, these E_a values imply that GPP rates increased faster (5.1-fold) than CR rates (2.7-
299 fold), in the Red Sea's thermal range (22–32.5 °C). These findings differ with the expected double
300 increase of heterotrophic respiration (regarding photosynthetic processes) with temperature (Harris et
301 al., 2006), but are closer to results obtained by Garcia-Corral et al. (2017), who recently reported E_a for
302 GPP of 0.86 , 1.48 and 1.07 eV for the Atlantic, Indian, and Pacific oceans, respectively, while E_a for
303 CR found in the Atlantic, Indian and the Pacific oceans were 0.77, 0.57 and 0.82 eV, respectively.

304 The apparent contradiction between our findings and the general patterns predicted by the MTE
305 is, however, not surprising. In their model, Allen et al. (2005) predict the activation energy of

306 photosynthesis per chloroplast (for temperatures between 0–30 °C) using the temperature dependence
307 parameters obtained by Bernacchi et al. (2001) for RuBisCO carboxylation rates in one species (tobacco
308 leaves). Although the temperature range selected by Allen et al. (2005) comprises the optimum
309 temperatures of growth rates for a wide range of functional groups of marine primary producers (Chen,
310 2015; Thomas et al., 2016), the temperature observed in the Red Sea exceeded this range. Due to the
311 fast generation times of microbes (Collins, 2010), we can expect that photosynthetic planktonic
312 communities are acclimated or even locally adapted to the thermal conditions they experience. So by
313 favouring certain photosynthetic or thermal traits, they can enhance their metabolism and growth to the
314 ambient temperature, up to their thermal optimum (Galmes et al., 2015; Thomas et al., 2016).
315 Therefore, it is likely that the acclimation or local adaptation (in the long term) of photosynthetic traits
316 in Red Sea plankton optimises the metabolic response at the high temperatures reached, resulting in a
317 steeper response to temperature than predicted by the MTE. Moreover, as the trait responses to
318 temperature vary among phylogenetic groups (Galmes et al., 2015; Galmés et al., 2016; Thomas et al.,
319 2016), we anticipated a certain degree of discrepancy if we characterise the photosynthetic response
320 (GPP) of planktonic communities by considering only one trait (i.e., RuBisCO carboxylation) of one
321 species.

322 However, we must bear in mind that the metabolic response of individuals is not only
323 temperature-dependent, and that resource supply also plays an essential role (Brown et al., 2004; Allen
324 and Gillooly, 2009). Our results evidenced that the increased response of planktonic metabolism
325 towards warmer temperatures was mostly confined to the southern half of the Red Sea, which receives
326 the direct inflow of the enriched Intermediate Water coming from the Gulf of Aden during the winter

327 monsoon (Raitsos et al., 2015; Wafar et al., 2016). Recent findings have demonstrated that mass-
328 specific carbon fixation rates of phytoplankton communities can be enhanced with increasing
329 temperature when nutrients are not limiting their growth (Marañón et al., 2014; Marañón et al., 2018).
330 Therefore, it is likely that the intertwined effect of both the warmer temperatures and the higher nutrient
331 availability towards the south of the Red Sea are key drivers regulating the metabolic response of
332 planktonic communities. Thus, unlike the global ocean, where nutrient concentration is inversely
333 correlated with temperature (e.g., Agawin et al. 2000), in the Red Sea nutrient concentration and
334 temperature are positively correlated. This anomaly may explain the steep increase in E_a for GPP, as
335 primary producers in the warmer region are being supported by the inflow of nutrient-enriched waters
336 from the Indian Ocean.

337 The elevated E_a for GPP compared to CR in Red Sea plankton is also an anomaly, likely
338 associated with the lack of allochthonous nutrient supply due to the absence of rivers and vegetation in
339 the arid watershed of the Red Sea. The warm oligotrophic ocean is characterised by plankton
340 communities that are in metabolic balance or net metabolically imbalanced (Duarte and Agusti 2008,
341 Duarte et al. 2013). In contrast, the warm Southern Red Sea tends to support autotrophic metabolism,
342 sustained by the input of nutrient-enriched waters while low allochthonous carbon inputs may constrain
343 CR. As a result, NCP tends to increase, rather than decrease with increasing temperature (Regaudie-de-
344 Gioux and Duarte 2011, Garcia-Corral et al. 2017). These patterns in plankton metabolism in the
345 oligotrophic and warm Red Sea deviate from those characterising the subtropical and tropical gyres of
346 the open ocean, but it provides an opportunity to explore the mechanistic basis for patterns in plankton

347 metabolism with temperature, which would otherwise remain obscured by the underlying prevalent
348 negative relationship with nutrient concentrations.

349 **5. Conclusions**

350 Our results show that plankton metabolism in the Red Sea presents a remarkably different
351 pattern compared to other warm and oligotrophic marine systems (e.g., the subtropical and tropical
352 gyres). In this region, autotrophic plankton communities prevailed and are supported by relatively high
353 GPP rates; above the threshold separating heterotrophic low-productivity communities from autotrophic
354 ones. Metabolically-balanced or net heterotrophic plankton communities dominated in the Northern Red
355 Sea, whereas autotrophic communities, were predominant in the south supported by nutrient inputs from
356 the Gulf of Aden. Elevated temperatures contributed to the enhanced metabolic activity of planktonic
357 organisms due to the increase in kinetic energy (favouring enzymatic reactions) with temperature.
358 Plankton communities in the Red Sea, however, displayed activation energies for GPP that were higher
359 than those for CR, resulting in a positive relationship between NCP and temperature. Those findings
360 represent anomalies in the relationship between metabolic rates and temperature compared to the warm,
361 oligotrophic open ocean. These anomalies are likely related to the higher nutrient supply from nutrient-
362 rich Indian Ocean waters in the warm Southern Red Sea, suggesting that GPP can respond strongly to
363 the temperature in the warm ocean when supported by high nutrient inputs, relative to those in the
364 subtropical gyres.

365

366 **Data availability**

367 The authors declare that the data supporting the findings are available within the article and from the
368 authors upon request.

369 **Author Contributions**

370 DCL-S, CMD, and SA designed the study; KR and PCdA obtained the data and provided technical
371 support; DCL-S cured and analysed the data; DCL-S wrote the article with a substantial contribution of
372 CMD, and SA; all authors discussed the results and commented on the manuscript.

373

374 **Competing interests**

375 The authors declare that they have no conflict of interests.

376 **Acknowledgements**

377 The authors thank the Editor and the reviewers for their thorough revision and constructive comments
378 that helped to greatly improve the manuscript. The research reported in this publication was supported
379 by funding from King Abdullah University of Science and Technology (KAUST), under award number
380 BAS/1/1071-01-10 assigned to CMD, BAS/1/1072-01-01 assigned to SA, and CCF/1/1973-21-01
381 assigned to the Red Sea Research Center.

- 383 Acker, J., Leptoukh, G., Shen, S., Zhu, T., and Kempner, S.: Remotely-sensed chlorophyll a observations of the northern Red Sea indicate
384 seasonal variability and influence of coastal reefs, *Journal of Marine Systems*, 69, 191-204, 10.1016/j.jmarsys.2005.12.006, 2008.
- 385 Agawin, N. S., Duarte, C. M., and Agustí, S.: Nutrient and temperature control of the contribution of picoplankton to phytoplankton biomass
386 and production, *Limnology and Oceanography*, 45, 591-600, 2000.
- 387 Al-aidaroos, A. M., Karati, K. K., El-sherbiny, M. M., Devassy, R. P., and Kürten, B.: Latitudinal environmental gradients and diel variability
388 influence abundance and community structure of Chaetognatha in Red Sea coral reefs, *Systematics and Biodiversity*, 15, 35-48,
389 10.1080/14772000.2016.1211200, 2016.
- 390 Almahasheer, H., Abdulaziz, A., and Duarte, C. M.: Decadal stability of Red Sea mangroves, *Estuarine Coastal and Shelf Science*, 169, 164-
391 172, 2016.
- 392 Almahasheer, H., Duarte, C. M., and Irigoien, X.: Leaf Nutrient Resorption and Export Fluxes of *Avicennia marina* in the Central Red Sea
393 Area, *Frontiers in Marine Science*, 5, 10.3389/fmars.2018.00204, 2018.
- 394 Allen, A., Gillooly, J., and Brown, J.: Linking the global carbon cycle to individual metabolism, *Functional Ecology*, 19, 202-213, 2005.
- 395 Allen, A. P., and Gillooly, J. F.: Towards an integration of ecological stoichiometry and the metabolic theory of ecology to better understand
396 nutrient cycling, *Ecol Lett*, 12, 369-384, 10.1111/j.1461-0248.2009.01302.x, 2009.
- 397 Barrón, C., and Duarte, C. M.: Dissolved organic carbon pools and export from the coastal ocean, *Global Biogeochemical Cycles*, 29, 1725-
398 1738, 2015.
- 399 Bender, M., Orchardo, J., Dickson, M.-L., Barber, R., and Lindley, S.: In vitro O₂ fluxes compared with 14 C production and other rate
400 terms during the JGOFS Equatorial Pacific experiment, *Deep Sea Research Part I: Oceanographic Research Papers*, 46, 637-654, 1999.
- 401 Bernacchi, C., Singaas, E., Pimentel, C., Portis Jr, A., and Long, S.: Improved temperature response functions for models of Rubisco-limited
402 photosynthesis, *Plant, Cell & Environment*, 24, 253-259, 2001.
- 403 Brown, J. H., Gillooly, J. F., Allen, A. P., Savage, V. M., and West, G. B.: Toward a metabolic theory of ecology, *Ecology*, 85, 1771-1789,
404 2004.
- 405 Carpenter, J. H.: The accuracy of the Winkler method for dissolved oxygen analysis, *Limnology and Oceanography*, 10, 135-140, 1965.
- 406 Clarke, A.: The influence of climate change on the distribution and evolution of organisms, *Animals and Temperature. Phenotypic and*
407 *Evolutionary Adaptation*, 377-407, 1996.
- 408 Collins, S.: Many Possible Worlds: Expanding the Ecological Scenarios in Experimental Evolution, *Evolutionary Biology*, 38, 3-14,
409 10.1007/s11692-010-9106-3, 2010.
- 410 Cullen, J.: Primary production methods, *Marine Ecology Progress Series*, 52, 88, 2001.
- 411 Chaidez, V., Dreano, D., Agustí, S., Duarte, C. M., and Hoteit, I.: Decadal trends in Red Sea maximum surface temperature, *Scientific*
412 *Reports*, 7, 8144, 10.1038/s41598-017-08146-z, 2017.
- 413 Chen, B.: Patterns of thermal limits of phytoplankton, *Journal of Plankton Research*, 37, 285-292, 10.1093/plankt/fbv009, 2015.
- 414 Chen, Y., Mills, S., Street, J., Golan, D., Post, A., Jacobson, M., and Paytan, A.: Estimates of atmospheric dry deposition and associated
415 input of nutrients to Gulf of Aqaba seawater, *Journal of Geophysical Research: Atmospheres*, 112, 2007.
- 416 Del Giorgio, P. A., Cole, J. J., and Cimleris, A.: Respiration rates in bacteria exceed phytoplankton production in unproductive aquatic
417 systems, *Nature*, 385, 148, 1997.
- 418 Duarte, C. M., and Agustí, S.: The CO₂ balance of unproductive aquatic ecosystems, *Science*, 281, 234-236, 1998.
- 419 Duarte, C. M., and Regaudie-de-Gioux, A.: Thresholds of gross primary production for the metabolic balance of marine planktonic
420 communities, *Limnology and Oceanography*, 54, 1015-1022, 2009.
- 421 Duarte, C. M., Regaudie-de-Gioux, A., Arrieta, J. M., Delgado-Huertas, A., and Agustí, S.: The Oligotrophic Ocean Is Heterotrophic, *Annual*
422 *Review of Marine Science*, 5, 551-569, 10.1146/annurev-marine-121211-172337, 2013.
- 423 Ducklow, H. W., Dickson, M.-L., Kirchman, D. L., Steward, G., Orchardo, J., Marra, J., and Azam, F.: Constraining bacterial production,
424 conversion efficiency and respiration in the Ross Sea, Antarctica, January–February, 1997, *Deep Sea Research Part II: Topical Studies in*
425 *Oceanography*, 47, 3227-3247, 2000.
- 426 Ducklow, H. W., and Doney, S. C.: What is the metabolic state of the oligotrophic ocean? A debate, *Ann Rev Mar Sci*, 5, 525-533,
427 10.1146/annurev-marine-121211-172331, 2013.
- 428 Engelbrecht, J. P., Stenichikov, G., Prakash, P. J., Lersch, T., Anisimov, A., and Shevchenko, I.: Physical and chemical properties of deposited
429 airborne particulates over the Arabian Red Sea coastal plain, *Atmospheric Chemistry and Physics*, 17, 11467-11490, 2017.
- 430 Galmes, J., Kapralov, M., Copolovici, L., Hermida-Carrera, C., and Niinemets, Ü.: Temperature responses of the Rubisco maximum
431 carboxylase activity across domains of life: phylogenetic signals, trade-offs, and importance for carbon gain, *Photosynthesis research*, 123,
432 183-201, 2015.

433 Galmés, J., Hermida-Carrera, C., Laanisto, L., and Niinemets, Ü.: A compendium of temperature responses of Rubisco kinetic traits:
434 variability among and within photosynthetic groups and impacts on photosynthesis modeling, *Journal of experimental botany*, 67, 5067-
435 5091, 2016.

436 García-Corral, L., Barber, E., Gioux, A. R. d., Sal, S., Holding, J., Agustí, S., Navarro, N., Serret, P., Mozeti, P., and Duarte, C.: Temperature
437 dependence of planktonic metabolism in the subtropical North Atlantic Ocean, *Biogeosciences*, 11, 4529-4540, 2014.

438 Garcia-Corral, L. S., Holding, J. M., Carrillo-de-Albornoz, P., Steckbauer, A., Pérez-Lorenzo, M., Navarro, N., Serret, P., Gasol, J. M.,
439 Morán, X. A. G., Estrada, M., Fraile-Nuez, E., Benítez-Barrios, V., Agusti, S., and Duarte, C. M.: Temperature dependence of plankton
440 community metabolism in the subtropical and tropical oceans, *Global Biogeochemical Cycles*, 31, 1141-1154, 10.1002/2017gb005629,
441 2017.

442 García-Martín, E. E., Daniels, C. J., Davidson, K., Davis, C. E., Mahaffey, C., Mayers, K. M. J., McNeill, S., Poulton, A. J., Purdie, D. A.,
443 Tarran, G. A., and Robinson, C.: Seasonal changes in plankton respiration and bacterial metabolism in a temperate shelf sea, *Progress in*
444 *Oceanography*, 10.1016/j.pocean.2017.12.002, 2017.

445 Garcias-Bonet, N., and Duarte, C. M.: Methane Production by Seagrass Ecosystems in the Red Sea, *Frontiers in Marine Science*, 4,
446 10.3389/fmars.2017.00340, 2017.

447 Gillooly, J. F., Brown, J. H., West, G. B., Savage, V. M., and Charnov, E. L.: Effects of size and temperature on metabolic rate, *science*,
448 293, 2248-2251, 2001.

449 Gillooly, J. F., Allen, A. P., West, G. B., and Brown, J. H.: The rate of DNA evolution: effects of body size and temperature on the molecular
450 clock, *Proceedings of the National Academy of Sciences of the United States of America*, 102, 140-145, 2005.

451 Hansen, H. P., and Koroleff, F.: Determination of nutrients, in: *Methods of seawater analysis*, edited by: K. Grasshoff, K. Kremling, and
452 Ehrhardt, M., Wiley-VCH Verlag, Weinheim, Germany, 159-228, 1999.

453 Harris, L. A., Duarte, C. M., and Nixon, S. W.: Allometric laws and prediction in estuarine and coastal ecology, *Estuaries and Coasts*, 29,
454 340-344, 2006.

455 Jurado, E., Dachs, J., Duarte, C. M., and Simo, R.: Atmospheric deposition of organic and black carbon to the global oceans, *Atmospheric*
456 *Environment*, 42, 7931-7939, 2008.

457 Kheireddine, M., Ouhssain, M., Claustre, H., Uitz, J., Gentili, B., and Jones, B.: Assessing pigment-based phytoplankton community
458 distributions in the Red Sea, *Frontiers in Marine Science*, 2017.

459 Kottuparambil, S., and Agusti, S.: PAHs sensitivity of picophytoplankton populations in the Red Sea, *Environmental Pollution*, 239, 607-
460 616, 2018.

461 Kürten, B., Al-Aidaros, A. M., Kürten, S., El-Sherbiny, M. M., Devassy, R. P., Struck, U., Zarokanellos, N., Jones, B. H., Hansen, T.,
462 Bruss, G., and Sommer, U.: Carbon and nitrogen stable isotope ratios of pelagic zooplankton elucidate ecohydrographic features in the
463 oligotrophic Red Sea, *Progress in Oceanography*, 140, 69-90, 10.1016/j.pocean.2015.11.003, 2016.

464 Levanon-Spanier, I., Padan, E., and Reiss, Z.: Primary production in a desert-enclosed sea—the Gulf of Elat (Aqaba), Red Sea, *Deep Sea*
465 *Research Part A. Oceanographic Research Papers*, 26, 673-685, 1979.

466 López-Sandoval, D. C., Delgado-Huertas, A., Carrillo-de-Albornoz, P., Duarte, C. M., and Agustí, S.: Use of cavity ring-down spectrometry
467 to quantify ¹³C-primary productivity in oligotrophic waters, *Limnology and Oceanography: Methods*, doi:10.1002/lom1003.10305,
468 doi:10.1002/lom3.10305, 2019.

469 López-Urrutia, Á., San Martín, E., Harris, R. P., and Irigoien, X.: Scaling the metabolic balance of the oceans, *Proceedings of the National*
470 *Academy of Sciences*, 103, 8739-8744, 2006.

471 Marañón, E., Cermeño, P., Huete-Ortega, M., López-Sandoval, D. C., Mouriño-Carballido, B., and Rodríguez-Ramos, T.: Resource supply
472 overrides temperature as a controlling factor of marine phytoplankton growth, *PLoS one*, 9, e99312, 2014.

473 Marañón, E., Lorenzo, M. P., Cermeño, P., and Mouriño-Carballido, B.: Nutrient limitation suppresses the temperature dependence of
474 phytoplankton metabolic rates, *The ISME journal*, 2018.

475 Osman, E. O., Smith, D. J., Ziegler, M., Kürten, B., Conrad, C., El-Haddad, K. M., Voolstra, C. R., and Suggett, D. J.: Thermal refugia
476 against coral bleaching throughout the northern Red Sea, *Global change biology*, 24, e474-e484, 2018.

477 Oudot, C., Gerard, R., Morin, P., and Gningue, I.: Precise shipboard determination of dissolved oxygen (Winkler procedure) for productivity
478 studies with a commercial system1, *Limnology and Oceanography*, 33, 146-150, 1988.

479 Padfield, D., Lowe, C., Buckling, A., Ffrench-Constant, R., Student Research, T., Jennings, S., Shelley, F., Olafsson, J. S., and Yvon-
480 Durocher, G.: Metabolic compensation constrains the temperature dependence of gross primary production, *Ecol Lett*, 20, 1250-1260,
481 10.1111/ele.12820, 2017.

482 Pearman, J. K., Kürten, S., Sarma, Y., Jones, B., and Carvalho, S.: Biodiversity patterns of plankton assemblages at the extremes of the Red
483 Sea, *FEMS microbiology ecology*, 92, fiw002, 2016.

484 Qurban, M. A., Balala, A. C., Kumar, S., Bhavya, P. S., and Wafar, M.: Primary production in the northern Red Sea, *Journal of Marine*
485 *Systems*, 132, 75-82, 10.1016/j.jmarsys.2014.01.006, 2014.

486 Qurban, M. A., Wafar, M., Jyothibabu, R., and Manikandan, K. P.: Patterns of primary production in the Red Sea, *Journal of Marine Systems*,
487 169, 87-98, 10.1016/j.jmarsys.2016.12.008, 2017.

488 Rahav, E., Herut, B., Mulholland, M. R., Belkin, N., Elifantz, H., and Berman-Frank, I.: Heterotrophic and autotrophic contribution to
489 dinitrogen fixation in the Gulf of Aqaba, *Marine Ecology Progress Series*, 522, 67-77, 2015.

490 Raitzos, D. E., Hoteit, I., Prihartato, P. K., Chronis, T., Triantafyllou, G., and Abualnaja, Y.: Abrupt warming of the Red Sea, *Geophysical*
491 *Research Letters*, 38, n/a-n/a, 10.1029/2011gl047984, 2011.

492 Raitzos, D. E., Pradhan, Y., Brewin, R. J., Stenchikov, G., and Hoteit, I.: Remote sensing the phytoplankton seasonal succession of the Red
493 Sea, *PLoS One*, 8, e64909, 10.1371/journal.pone.0064909, 2013.

494 Raitzos, D. E., Yi, X., Platt, T., Racault, M.-F., Brewin, R. J. W., Pradhan, Y., Papadopoulos, V. P., Sathyendranath, S., and Hoteit, I.:
495 Monsoon oscillations regulate fertility of the Red Sea, *Geophysical Research Letters*, 42, 855-862, 10.1002/2014gl062882, 2015.

496 Rasul, N. M., and Stewart, I. C.: *The Red Sea: the formation, morphology, oceanography and environment of a young ocean basin*, Springer,
497 2015.

498 Rasul, N. M., Stewart, I. C., and Nawab, Z. A.: Introduction to the Red Sea: its origin, structure and environment., in: *The Red Sea*, edited
499 by: Rasul, N. M., and Stewart, I. C., Springer, Berlin, 1-28, 2015.

500 Regaudie-de-Gioux, A., and Duarte, C. M.: Temperature dependence of planktonic metabolism in the ocean, *Global Biogeochemical Cycles*,
501 26, 2012.

502 Regaudie-de-Gioux, A., and Duarte, C. M.: Global patterns in oceanic planktonic metabolism, *Limnology and Oceanography*, 58, 977-986,
503 doi:10.4319/lo.2013.58.3.0977, 2013.

504 Robinson, C., and Williams, P. J. I. B.: Plankton net community production and dark respiration in the Arabian Sea during September 1994,
505 *Deep Sea Research Part II: Topical Studies in Oceanography*, 46, 745-765, 1999.

506 Robinson, C., Serret, P., Tilstone, G., Teira, E., Zubkov, M. V., Rees, A. P., and Woodward, E. M. S.: Plankton respiration in the eastern
507 Atlantic Ocean, *Deep Sea Research Part I: Oceanographic Research Papers*, 49, 787-813, 2002.

508 Robinson, C., and Williams, P. J. I. B.: Respiration and its measurement in surface marine waters, *Respiration in aquatic ecosystems*, 147-180,
509 2005.

510 Robitzsch, V. S., Lozano-Cortes, D., Kandler, N. M., Salas, E., and Berumen, M. L.: Productivity and sea surface temperature are correlated
511 with the pelagic larval duration of damselfishes in the Red Sea, *Mar Pollut Bull*, 105, 566-574, 10.1016/j.marpolbul.2015.11.045, 2016.

512 Serret, P., Robinson, C., Fernández, E., Teira, E., and Tilstone, G.: Latitudinal variation of the balance between plankton photosynthesis and
513 respiration in the eastern Atlantic Ocean, *Limnology and Oceanography*, 46, 1642-1652, 2001.

514 Serret, P., Robinson, C., Fernández, E., Teira, E., Tilstone, G., and Pérez, V.: Predicting plankton net community production in the Atlantic
515 Ocean, *Deep Sea Research Part II: Topical Studies in Oceanography*, 56, 941-953, 2009.

516 Smith, S., and Mackenzie, F.: The ocean as a net heterotrophic system: implications from the carbon biogeochemical cycle, *Global*
517 *Biogeochemical Cycles*, 1, 187-198, 1987.

518 Smith, S., and Hollibaugh, J.: Coastal metabolism and the oceanic organic carbon balance, *Reviews of Geophysics*, 31, 75-89, 1993.

519 Sofianos, S., and Johns, W. E.: Water mass formation, overturning circulation, and the exchange of the Red Sea with the adjacent basins, in:
520 *The Red Sea*, Springer, 343-353, 2015.

521 Sofianos, S. S.: An Oceanic General Circulation Model (OGCM) investigation of the Red Sea circulation, 1. Exchange between the Red Sea
522 and the Indian Ocean, *Journal of Geophysical Research*, 107, 10.1029/2001jc001184, 2002.

523 Sofianos, S. S., and Johns, W. E.: Observations of the summer Red Sea circulation, *Journal of Geophysical Research*, 112,
524 10.1029/2006jc003886, 2007.

525 Thomas, M. K., Kremer, C. T., and Litchman, E.: Environment and evolutionary history determine the global biogeography of phytoplankton
526 temperature traits, *Global Ecology and Biogeography*, 25, 75-86, 10.1111/geb.12387, 2016.

527 Tilstra, A., van Hoytema, N., Cardini, U., Bednarz, V. N., Rix, L., Naumann, M. S., Al-Horani, F. A., and Wild, C.: Effects of water column
528 mixing and stratification on planktonic primary production and dinitrogen fixation on a northern Red Sea coral reef, *Frontiers in*
529 *microbiology*, 9, 2018.

530 Torfstein, A., and Kienast, S.: No Correlation Between Atmospheric Dust and Surface Ocean Chlorophyll-a in the Oligotrophic Gulf of
531 Aqaba, Northern Red Sea, *Journal of Geophysical Research: Biogeosciences*, 123, 391-405, 2018.

532 Wafar, M., Qurban, M. A., Ashraf, M., Manikandan, K., Flandez, A. V., and Balala, A. C.: Patterns of distribution of inorganic nutrients in
533 Red Sea and their implications to primary production, *Journal of Marine Systems*, 156, 86-98, 2016.

534 Williams, P., Raine, R. C. T., and Bryan, J. R.: Agreement between the c-14 and oxygen methods of measuring phytoplankton production-
535 reassessment of the photosynthetic quotient, *Oceanologica Acta*, 2, 411-416, 1979.

536 Williams, P.: On the definition of plankton production terms, *ICES marine science symposia*. 1993., 1993,

537 Williams, P. I. B.: The balance of plankton respiration and photosynthesis in the open oceans, *Nature*, 394, 55-57, 1998.

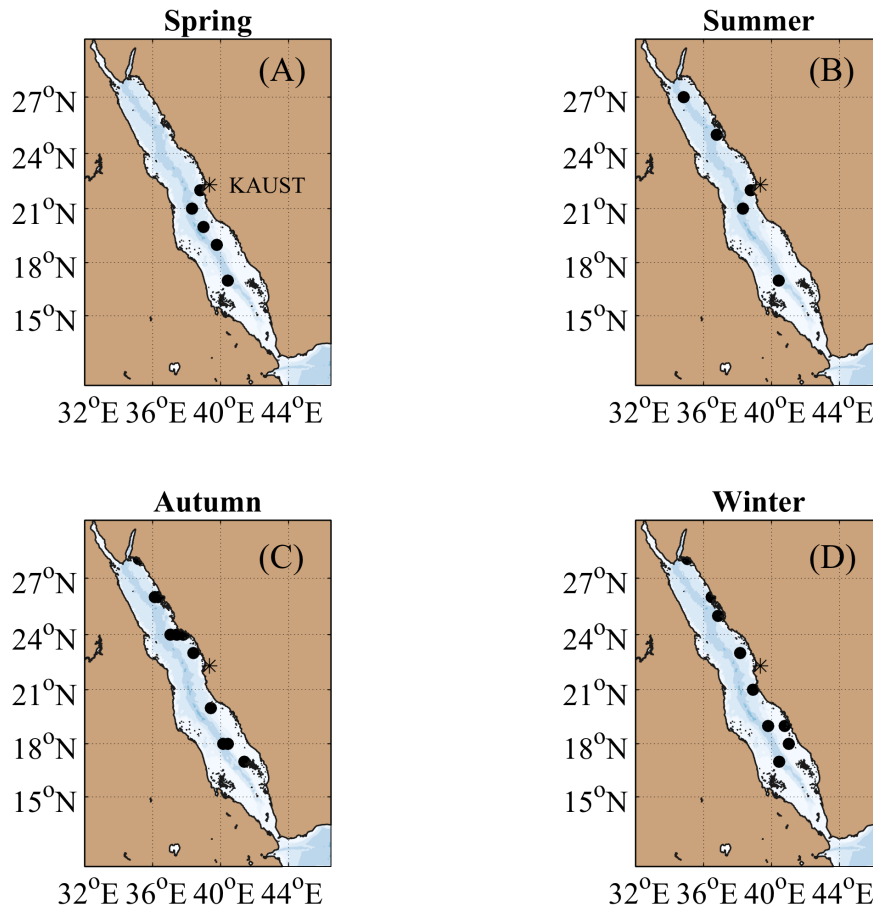
538 Williams, P. I. B., and del Giorgio, P. A.: Respiration in aquatic ecosystems: history and background, *Respiration in aquatic ecosystems*, 1-
539 17, 2005.

540 Zarokanellos, N., Papadopoulos, V. P., Sofianos, S., and Jones, B.: Physical and biological characteristics of the winter-summer transition
541 in the Central Red Sea, *Journal of Geophysical Research: Oceans*, 122, 6355-6370, <http://dx.doi.org/10.1002/2017jc012882>, 2017.

542

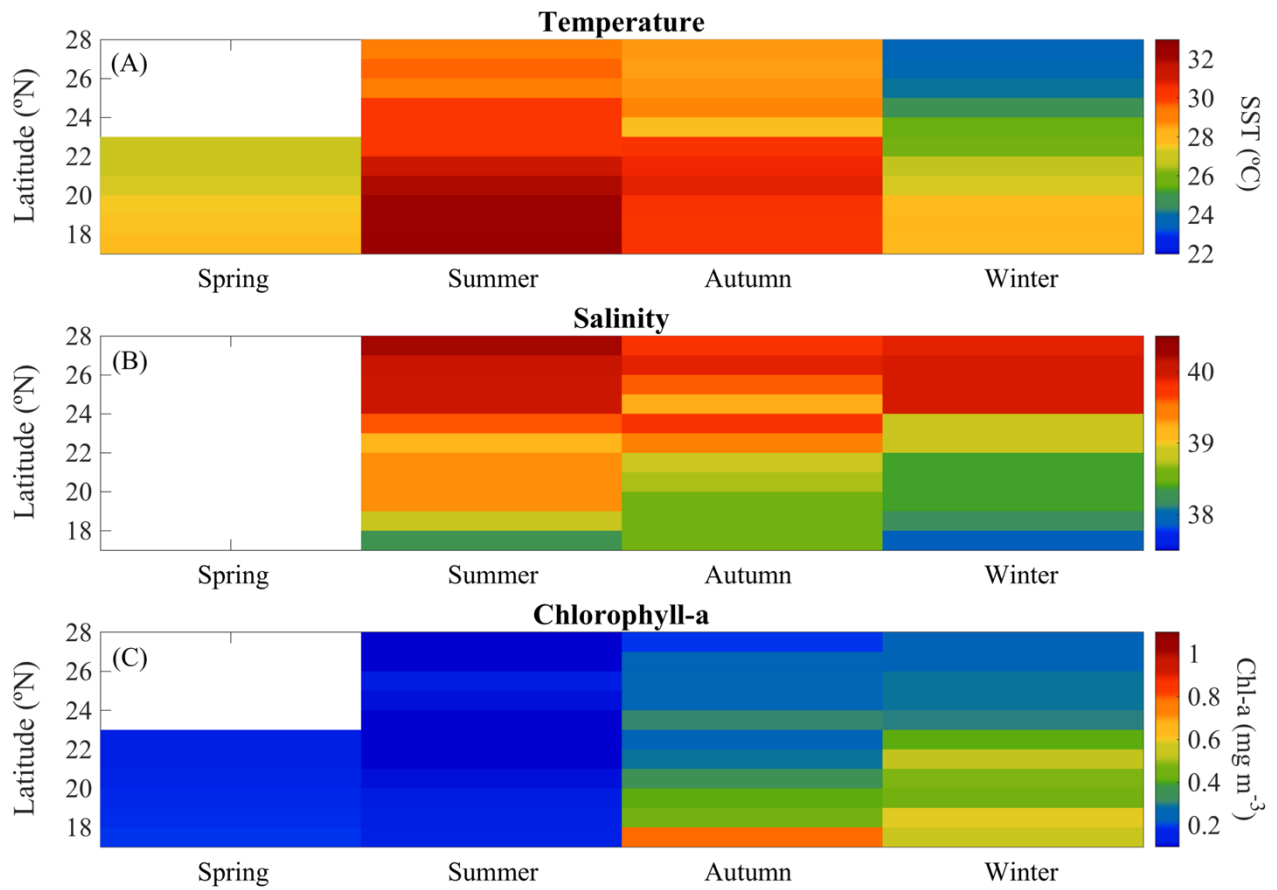
543

544 The logo of Copernicus Publication



545

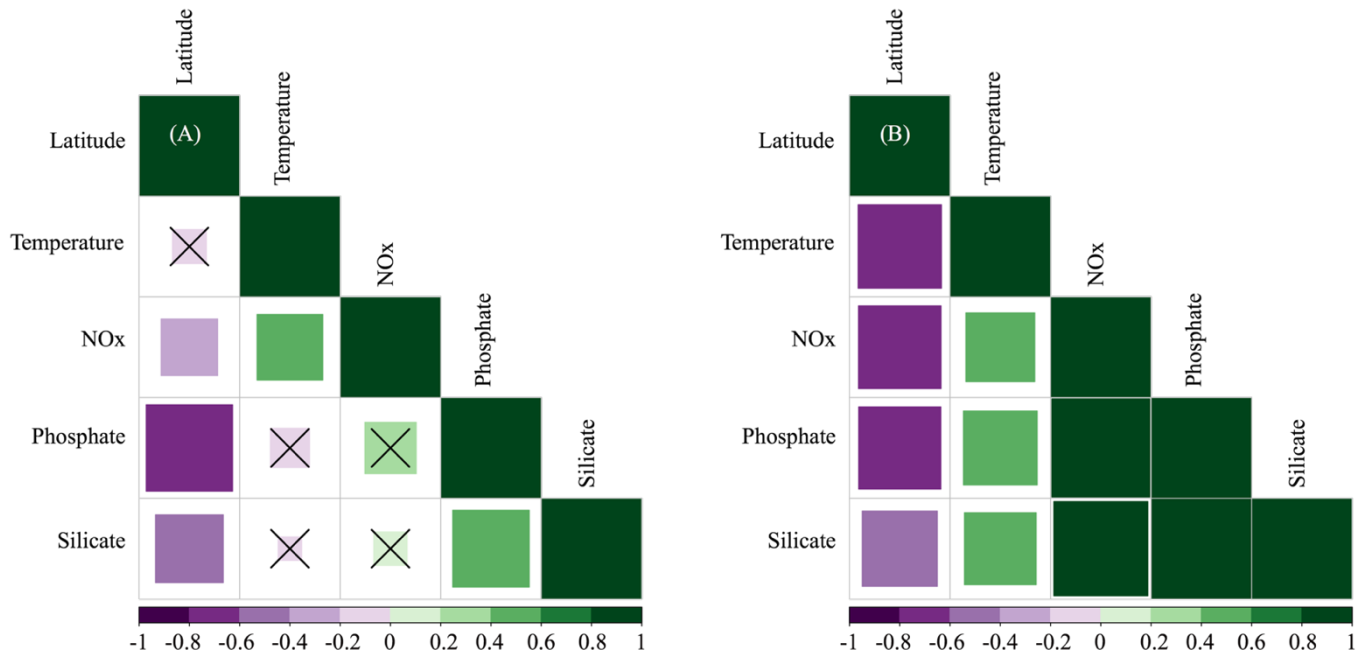
Figure 1: Stations sampled along the Red Sea during (A) spring (2018), (B) summer 2018, (C) autumn (2016) and (D) winter 2016 and 2017



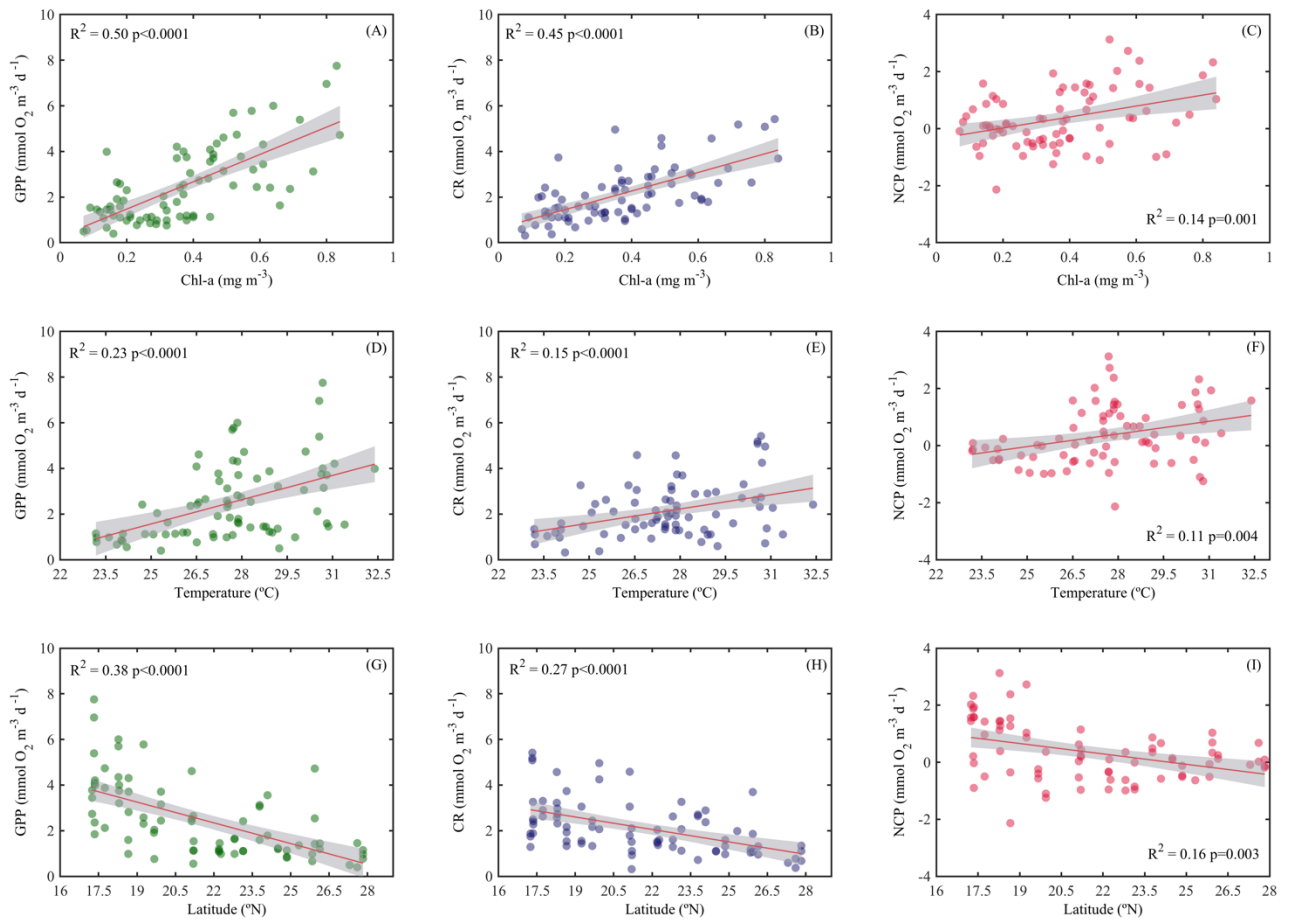
550

Figure 2: Overall seasonal and latitudinal variability of surface (A) temperature (SST), (B) salinity (C) and chlorophyll-a concentration (Chl-a) measured during spring (2018), summer (2017), autumn (2016) and winter (2016 and 2017) cruises along the Red Sea (~ 100% of incident Photosynthetically Active Radiation, PAR).

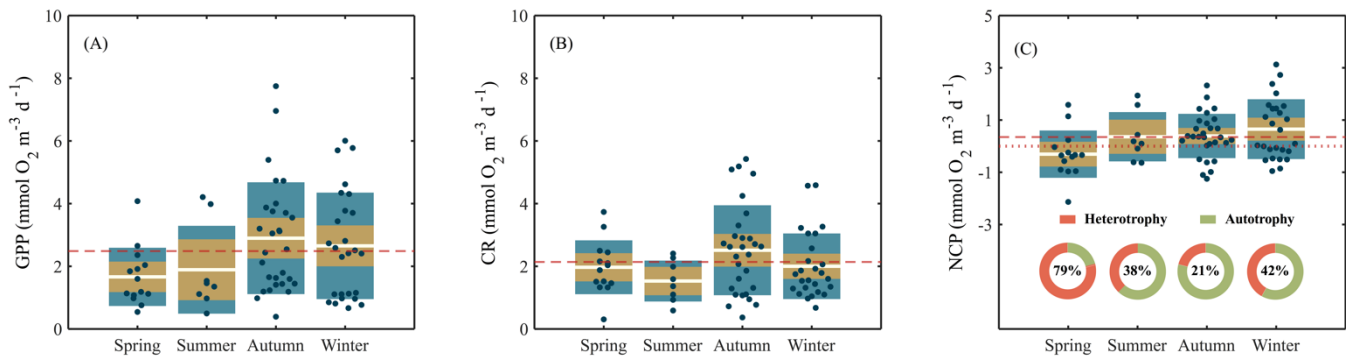
555



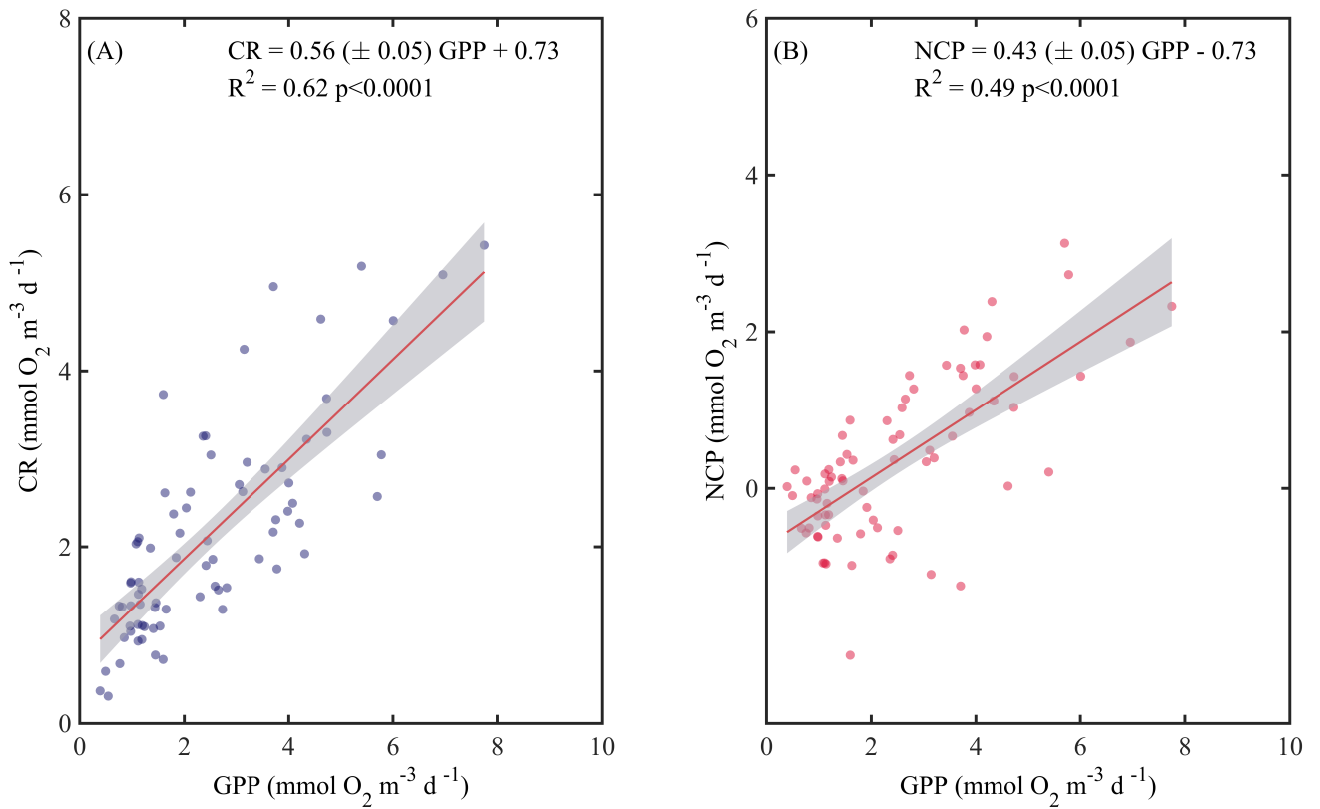
560 Figure 3: Pearson correlations between environmental variables (temperature and the concentrations of
 565 nitrate+nitrite [NOx], phosphate and silicate) and their latitudinal distribution measured at selected
 depths: (A) the first optical depth (from the surface down to 37% of incident PAR) and (B) at the
 bottom of the photic layer (between 1–0.1% of incident PAR values). The size of the squares is the
 magnitude, the color indicates the direction (green for positive correlations, purple for negative
 correlations). The value of the correlation coefficient (r) is shown in the color bar below the graphs.
 Non-significant correlations are denoted with a \times .



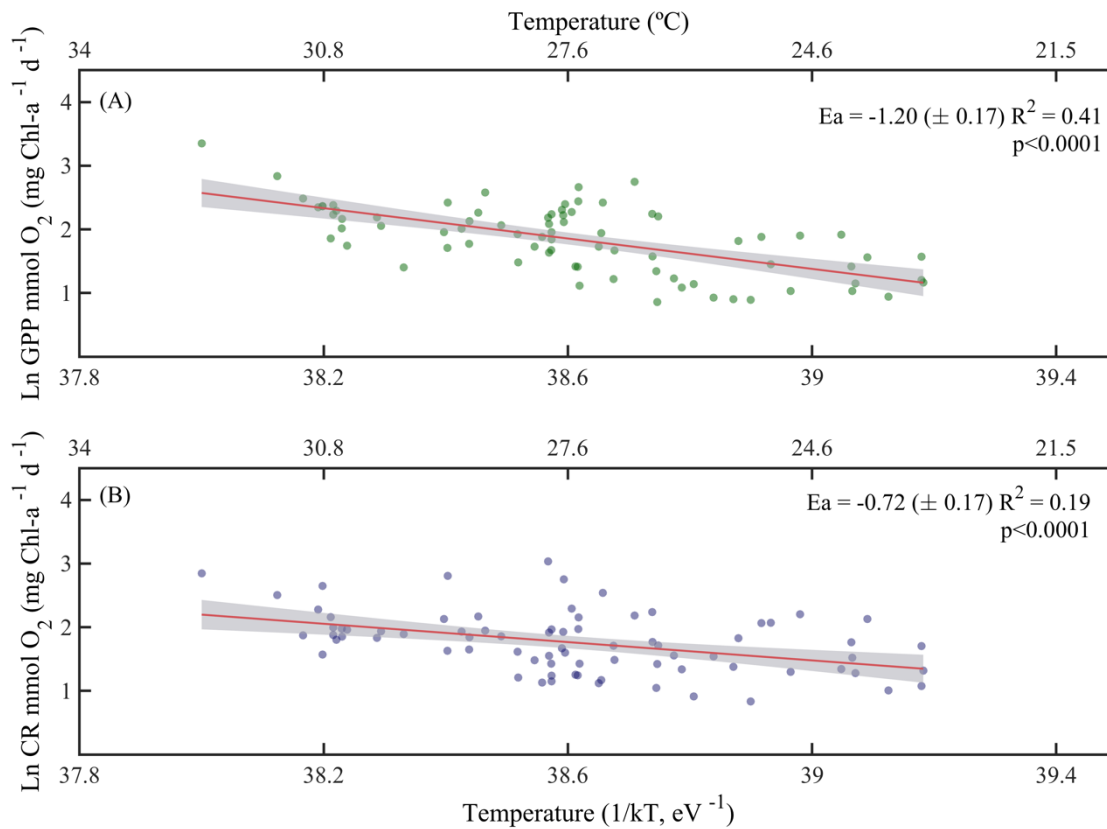
570 Figure 4: Ordinary least squares linear regression between gross primary production (GPP), planktonic community respiration (CR) and net community production rates (NCP) with (A, B, C) Chlorophyll-a concentration (Chl-a), (D, E, F) temperature and (G, H, I) latitude. The solid red line is the linear least square fit, while the shaded grey area represents the 95% confidence intervals. The coefficient of determination and the statistical significance are indicated for each regression.



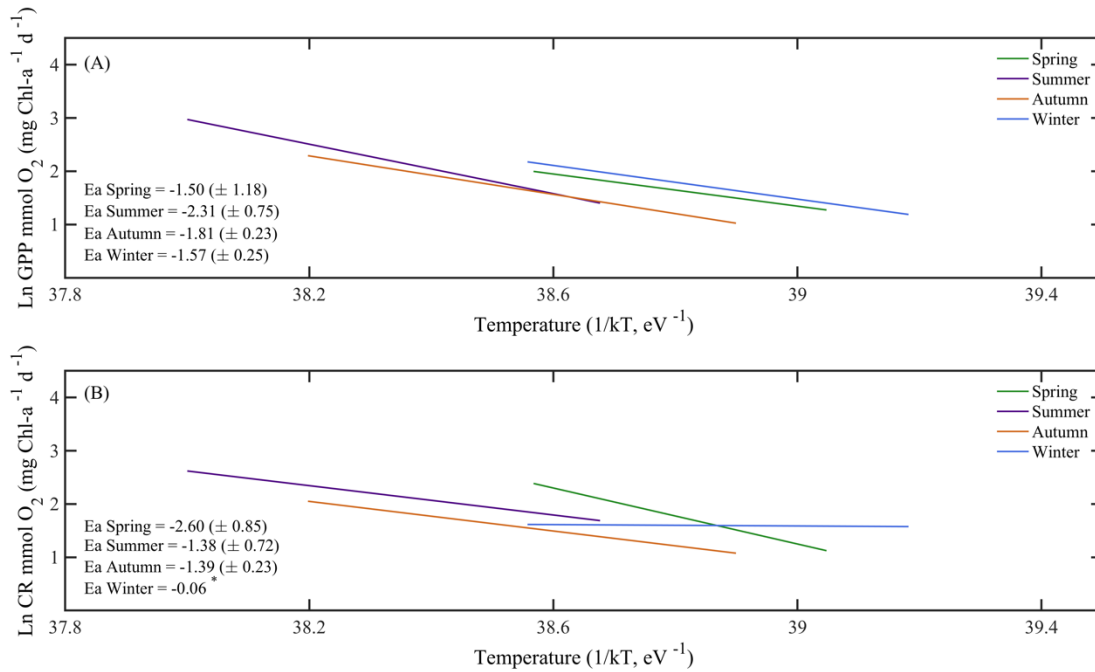
575 Figure 5. Seasonal variability of (A) gross primary production (GPP), (B) community respiration (CR),
 and (C) net community production (NCP) measured along the Red Sea. Boxplots indicate the 95%
 confidence intervals (in lighter colour), and ± 1 SD (dark shaded). The central horizontal white lines in
 the box mark the mean value for each season. The red dashed lines represent the overall mean while the
 red dotted line in (C) defines the limit between autotrophic from heterotrophic communities (NCP=0).
 580 Values inside the donut plots (C) indicate the percentage of heterotrophy (NCP<) for each season.



585 Figure 6: Ordinary least square linear regression between (A) planktonic community respiration and (B) net community production (NCP) with gross primary production (GPP) rates measured along the Red Sea. The ordinary least square regression parameters (slope and intercept) and the statistical significance of each regression are indicated. The solid red line represents the linear least square fit, the shaded grey area represents the 95% confidence interval.



590 Figure 7: Arrhenius plots indicating temperature dependence of planktonic metabolic rates plotted as the
 595 relationship between the natural logarithm of (A) chlorophyll-a normalised gross primary production,
 and (B) chlorophyll-a normalised planktonic community respiration with temperature as a function of
 $1/kT$ (lower axis), where k is the Boltzmann's constant ($8.2 \times 10^{-5} \text{ eV K}^{-1}$), and T denotes the absolute
 temperature (K). The corresponding temperatures in degree Celsius are shown in the upper axis for each
 graph. The solid red line is the linear least square fit, the shaded grey area represents the 95%
 confidence interval. E_a represents the activation energy ($E_a = -\text{slope}$).



600 Figure 8: Arrhenius plots indicating the seasonal temperature dependence of planktonic metabolic rates plotted as the relationship between the natural logarithm of (A) chlorophyll-*a* normalised gross primary production, and (B) planktonic community respiration with temperature as a function of $1/kT$ (lower axis), where k is the Boltzmann's constant ($8.2 \times 10^{-5} \text{ eV K}^{-1}$), and T denotes the absolute temperature (K). Each line represents the linear least square fit. E_a represents the activation energy ($E_a = -\text{slope}$).

605

610

615

620 Table 1. Pearson correlation matrix between volumetric gross primary production (GPP), planktonic
community respiration (CR) and net community production (NCP) with environmental variables
(temperature; latitude; nitrite+nitrate, NO_x; and Chlorophyll-a concentration, Chl-*a*). Bold numbers
indicate significant relationships and the significance level is indicated with *: p<0.05*, p<0.01** and
p<0.001***.

625

	Temperature	Latitude	NO _x	Chl- <i>a</i>	GPP	CR	NCP
GPP	0.5***	-0.6***	0.0	0.7***		0.8***	0.7***
CR	0.4***	-0.5***	0.2	0.7***	0.8***		0.1
NCP	0.3**	-0.4***	-0.1	0.4***	0.7***	0.1	
Chl- <i>a</i>	0.1	-0.4***	0.3*		0.7***	0.7***	0.4**